

See discussions, stats, and author profiles for this publication at: <https://www.researchgate.net/publication/231274684>

Fractal Characterization of Spontaneous Co-current Imbibition in Porous Media

ARTICLE *in* ENERGY & FUELS · FEBRUARY 2010

Impact Factor: 2.79 · DOI: 10.1021/ef901413p

CITATIONS

67

READS

76

4 AUTHORS, INCLUDING:



Jianchao Cai

China University of Geosciences

52 PUBLICATIONS 639 CITATIONS

SEE PROFILE



Boming Yu

Huazhong University of Science and Technol...

130 PUBLICATIONS 2,693 CITATIONS

SEE PROFILE

Fractal Characterization of Spontaneous Co-current Imbibition in Porous Media

Jianchao Cai, Boming Yu,* Mingqing Zou, and Liang Luo

School of Physics, Huazhong University of Science and Technology, Wuhan 430074, Hubei, People's Republic of China

Received November 19, 2009. Revised Manuscript Received January 26, 2010

Spontaneous capillary imbibition is an important fundamental phenomenon existing extensively in a variety of processes such as polymer composite manufacturing, oil recovery, soil science and hydrology, etc. In this work, analytical expressions for characterizing a spontaneous co-current imbibition process of wetting fluid into gas-saturated porous media are proposed based on the fractal characters of porous media. The mass of imbibed liquid is expressed as a function of the fractal dimensions for pores and for tortuous capillaries, the minimum and maximum hydraulic diameter of pores, and the ratio for minimum to maximum hydraulic diameters, porosity, and fluid properties, as well as the fluid–solid interaction. The imbibed weight predicted by the present model is in good agreement with the available experimental data.

1. Introduction

There is an increasing interest in precisely evaluating the magnitude and role of the capillary effect in infiltration processing, because spontaneous capillary imbibition is an important fundamental phenomenon existing extensively in a variety of processes such as oil recovery, polymer composite manufacturing, soil science and hydrology, etc. It is generally found that the contact angle of liquid against air measured statically is lower than 90° in most oil and gas reservoirs¹ and, in most cases, in polymer composites.² Thus, the capillary suction will draw wetting liquid into porous media (e.g., rock matrix or fabrics). Study of spontaneous imbibition is essential not only in evaluating the wettability of the solid–liquid systems,³ but also in predicting the production performance in these oil/gas reservoirs developed by water flooding.⁴ The rate of imbibition is usually related to microstructures of porous media, fluid properties and their interactions, such as absolute and relative permeability,⁴ shapes and boundary conditions,^{5,6} viscosity,^{7,8} initial water saturation,^{9,10} interfacial tension,¹¹ and wettability.^{3,12}

In oil recovery, the surface tension of drilling and completion fluids was often designed as small as possible to reduce formation damage. Similarly, in the polymer composite industry, the surface tension of polymers was thought to be low.² Therefore, the capillary pressure drop was usually assumed to be smaller than the applied pressure, and the capillary effects were often neglected with regard to the oil recovery and polymer composite. However, some other investigators noticed the role of the capillary effect in oil recovery^{4,5,13} and in composite processing,^{2,14} and they found that, even if the effect is low in magnitude, it exerts a significant effect on void formation during the imbibition of porous media.²

In early studies, Washburn¹⁵ theoretically analyzed the spontaneous water imbibition and proposed a simple cylindrical model, in which the porous medium is represented by a collection of parallel tubes, each having the same radius. However, the sizes of pores in natural porous media vary from point to point and are even found to extend several orders of magnitude. Clearly, this model could not properly quantify the capillary imbibition process, because of the complex structure of natural porous media. Lundblad and Bergman¹⁶ introduced the effective radius by taking the tortuosity of capillaries into account and investigated the capillary rising in a porous electrode. In their model, the effective radius must be estimated for each capillary by measuring the wetting rate with a liquid of known contact angle. Some theoretical models describe the capillary imbibition by taking into account different geometrically shaped pores;¹⁷ as stated by Benavente et al.,¹⁸ these models were constructed to have a simple mathematical formulation, but they presented a poor agreement with the actual pore structure, and the results were sometimes in poor agreement with experimental data. Benavente et al.¹⁸ modified

*Author to whom correspondence should be addressed. Tel.: 86-27-87542153. E-mail: yuboming2003@yahoo.com.cn.

(1) Bear, J. *Dynamics of Fluids in Porous Media*; Elsevier: New York, 1972.

(2) Verrey, J.; Michaud, V.; Manson, J. A. E. *Composites—Part A* **2006**, 37, 92–102.

(3) Ma, S.; Morrow, N. R.; Zhou, X.; Zhang, X. Paper CIM 94-47. Presented at the 45th Annual Technical Meeting of the Petroleum Society of CIM, Calgary, Canada, June 12–15, 1994.

(4) Li, K. W.; Horne, R. N. *SPE J.* **2001**, 6, 375–384.

(5) Zhang, X.; Morrow, N. R.; Ma, S. *SPE Res. Eng.* **1996**, (Nov.), 280–285.

(6) Standnes, D. C. *Energy Fuels* **2004**, 18, 271–282.

(7) Ma, S.; Zhang, X.; Morrow, N. R. Paper CIM 95-94. Presented at the 46th Annual Technical Meeting of the Petroleum Society of CIM, Banff, Alberta, Canada, May 14–17, 1995.

(8) Standnes, D. C. *Energy Fuels* **2009**, 23, 2149–2156.

(9) Schembre, J. M.; Akin, S.; Castanier, L. M.; Kovscek, A. R. *SPE Paper No. 46211*. Presented at the 1998 Western Regional Meeting, Bakerfield, CA, May 10–13, 1998.

(10) Puntervold, T.; Strand, S.; Austad, T. *Energy Fuels* **2007**, 21, 3425–3430.

(11) Hognesen, E. J.; Standnes, D. C.; Austad, T. *Energy Fuels* **2004**, 18, 1665–1675.

(12) Zhang, P. M.; Tveheyo, M. T.; Austad, T. *Energy Fuels* **2006**, 20, 2056–2062.

(13) Handy, L. L. *Pet. Trans. AIME* **1960**, 219, 75–80.

(14) Amico, S. C.; Lekakou, C. *Polym. Compos.* **2002**, 23, 249–263.

(15) Washburn, E. W. *Phys. Rev.* **1921**, 17, 273–283.

(16) Lundblad, A.; Bergman, B. J. *Electrochem. Soc.* **1997**, 144, 984–987.

(17) Leventis, A.; Verganelakis, D. A.; Halse, M. R.; Webber, J. B.; Strange, J. H. *Transp. Porous Media* **2000**, 39, 143–157.

(18) Benavente, D.; Lock, P.; Angeles García Del Cura, M.; Ordóñez, S. *Transp. Porous Media* **2002**, 49, 59–76.

the Lucas–Washburn (LW) equation^{15,19} by introducing various corrections relating to the microstructures (tortuosity and pore shape) of the rocks. In their model, the introduced tortuosity (which is equal to 3) is considered as an empirical constant; this assumption was not reliable, because the tortuosity usually varies with effective porosity and microstructures of porous media.²⁰ In addition, their model predictions also were not in good agreement with their experimental data.

On the other hand, Handy¹³ presented an expression to characterize the process of spontaneous water imbibition into gas-saturated rocks (gas–liquid–rock systems) by neglecting gravity and assuming pistonlike displacement of imbibition process and infinite mobility of the gas phase, and the model is

$$W^2 = \rho^2 A^2 \left(\frac{P_c K \phi S_{wf}}{\mu} \right) t \quad (1)$$

where W is the mass of wetting fluid imbibed, A the cross-sectional area of the core, ϕ the porosity, ρ the density, μ the viscosity, and t the time. The variables K , P_c , and S_{wf} are, respectively, the effective permeability, the capillary pressure, and the wetting phase saturation. However, according to eq 1, the amount of water imbibed into porous media is infinite when imbibition time approaches infinity, and this is physically impossible for all systems, not only systems that are mounted vertically. In addition, permeability and capillary pressure cannot be determined separately from a spontaneous water imbibition test;⁴ thus, both parameters must be measured separately.

Li and Horne,⁴ from their experimental results, concluded that gravitational forces should not be neglected in many cases, depending on the ratio of gravity to the capillary pressure gradient. They modified eq 1 by taking into account the gravity, based on the hypothesis that the spontaneous imbibition of water vertically rising in a core sample follows Darcy's law, and thus the infinite value from eq 1 would not appear. In addition, permeability and capillary pressure can also be calculated separately from test data, using their proposed semiempirical correlations for water imbibition into porous media.

There are also many other reports on experimental studies of spontaneous imbibition of water into oil-wet rock systems, taking into account the effect of surface-active chemicals,^{11,21,22} brine salinity and composition,²³ and temperature on the oil recovery.²⁴ However, study²⁵ of the spontaneous imbibition process, based on the fractal characters of porous media, was limited. In the work by Zhao and Li,²⁵ they proposed a fractal model to predict a power law relationship between spontaneous imbibition rate and time. It has been shown that the pore space of natural porous media is fractal and tortuous

streamtubes/capillaries^{26,27} in natural porous media also exhibit the fractal behavior. The velocity of the wetting liquid is dependent on the radii of cylindrical tubes, and there is also a pressure difference between the liquid in different tubes at a fixed distance from the inlet. To overcome this difficulty, the perfect cross-flow model was introduced by Dong et al.²⁸ and independently by Ruth and Bartley²⁹ (also see the review in ref 30). In this work, we assume that porous media are comprised of a bundle of independent differently sized parallel capillaries. Based on this assumption, this work attempts to apply the fractal geometry to derive an analytical expression for characterizing the physical process of spontaneous capillary imbibition into air-saturated porous media and only the co-current imbibition (i.e., the flowing direction of the wetting phase is the same as that of the nonwetting phase) is considered. According to analysis of the method used to measure the surface energy of powders,³¹ the viscosity and density factors of gas are neglected in this work. For this purpose, the next section is devoted to briefly introducing the fractal characters of porous media, and then in section 3, a model for spontaneous imbibition in porous media is derived, including the effect of gravity. The results and discussions are presented in section 4, and concluding remarks are given in section 5.

2. Fractal Characters of Porous Media

Since the fractal geometry theory introduced by Mandelbrot,³² the fractal geometry has been shown to be powerful in a variety of fields, such as polymer composite manufacturing, oil recovery, groundwater flow, chemistry, physics, material sciences, and soil science. Many researchers studied the transport properties and fractal natures in porous media over the past three decades.^{26,33–40} To analyze the spontaneous water imbibition into a porous medium, the basic fractal characteristics are briefly introduced as follows. Generally, natural porous media exhibit fractal behavior only in a limited range of length scales.^{33,41,42} The lower and upper limits of this domain of self-similarity can be identified with the corresponding limits of the pore sizes λ_{\min} and λ_{\max} , respectively. The pores that do not follow the fractal behavior are not concerned in the present work.

- (19) Lucas, R. *Kolloid-Z.* **1918**, 23, 15–22.
- (20) Barrande, M.; Bouchet, R.; Denoyel, R. *Anal. Chem.* **2007**, 79, 9115–9121.
- (21) Standnes, D. C.; Austad, T. J. *Pet. Sci. Eng.* **2000**, 28, 123–143.
- (22) Standnes, D. C.; Nogaret, L. A. D.; Chen, H. L.; Austad, T. *Energy Fuels* **2002**, 16, 1557–1564.
- (23) Strand, S.; Standnes, D. C.; Austad, T. *Energy Fuels* **2003**, 17, 1133–1144.
- (24) Strand, S.; Puntervold, T.; Austad, T. *Energy Fuels* **2008**, 22, 3222–3225.
- (25) Zhao, H. Y.; Li, K. W. SPE Paper No. 119525. Presented at the *Latin American and Caribbean Petroleum Engineering Conference*, Cartagena, Colombia, May 31–June 3, 2009.
- (26) Wheatcraft, S. W.; Tyler, S. W. *Water Resour. Res.* **1988**, 24, 566–578.

- (27) Majumdar, A. *Annu. Rev. Heat Transfer* **1992**, 4, 51–110.
- (28) Dong, M.; Dullien, F. A. L.; Zhou, J. *Transp. Porous Media* **1998**, 31, 213–237.
- (29) Ruth, D.; Bartley, J. Paper No. SCA2002-15. In *Proceedings of the 2002 International Symposium of the Society of Core Analysts*, Monterey, CA; 2003; p 12.
- (30) Unsal, E.; Mason, G.; Ruth, D. W.; Morrow, N. R. *J. Colloid Interface Sci.* **2007**, 315, 200–209.
- (31) Dunstan, D.; White, L. R. *J. Colloid Interface Sci.* **1986**, 111, 60–64.
- (32) Mandelbrot, B. B. *Fractals: Form, Chance and Dimension*; W.H. Freeman: San Francisco, CA, 1977.
- (33) Katz, A. J.; Thompson, A. H. *Phys. Rev. Lett.* **1985**, 54, 1325–1328.
- (34) Krohn, C. E.; Thompson, A. H. *Phys. Rev. B* **1986**, 33, 6366–6374.
- (35) Majumdar, A.; Bhushan, B. *ASME J. Tribol.* **1990**, 112, 205–216.
- (36) Perfect, E.; Blevins, R. L. *Soil Sci. Soc. Am. J.* **1997**, 61, 896–900.
- (37) Yu, B. M.; Li, J. H. *Fractals* **2001**, 9, 365–372.
- (38) Yu, B. M.; Cheng, P. *Int. J. Heat Mass Transfer* **2002**, 45, 2983–2993.
- (39) Yu, B. M. *Chin. Phys. Lett.* **2005**, 22, 158–160.
- (40) Yu, B. M. *Appl. Mech. Rev.* **2008**, 61, 050801.
- (41) Thompson, A. H.; Katz, A. J.; Krohn, C. E. *Adv. Phys.* **1987**, 36, 625–694.
- (42) Krohn, C. E. *J. Geophys. Res.* **1988**, 93, 3297–3305.

For a fractal porous medium, the number of pores whose sizes are within the infinitesimal range from λ to $\lambda + d\lambda$ is given as^{35,38}

$$-dN = D_f \lambda_{\max}^{D_f} \lambda^{-(D_f+1)} d\lambda \quad (2)$$

and the probability density function for pores is given by

$$f(\lambda) = D_f \lambda_{\min}^{D_f} \lambda^{-(D_f+1)} \quad (3)$$

with $\lambda_{\min} \leq \lambda \leq \lambda_{\max}$, where λ is the pore size, the fractal dimension D_f for pores in porous media is in the range of $0 < D_f < 2$ and $0 < D_f < 3$ in the two-dimensional (2D) and three-dimensional (3D) spaces, respectively. For simplicity, the ratio β is defined in this work as $\beta = \lambda_{\min}/\lambda_{\max}$ and, generally, in porous media, it has a value of $\beta \leq 10^{-2}$.

Pores with various sizes arbitrarily locate in a natural porous medium and form tortuous channels for fluid flow. In this work, porous media are assumed to be comprised of a bundle of tortuous capillaries/channels with different cross-sectional areas, with diameter and tortuous length being given as λ and $h_f(\lambda)$, respectively. The fractal dimension for tortuous stream tubes for flow through heterogeneous porous media can be described by $h_f(\varepsilon) = \varepsilon^{1-D_T} h_0^{D_T}$.²⁶ Yu and Cheng³⁸ argued that the diameter (λ) of tortuous capillaries is analogous to the length scale (ε) of measurement and developed the fractal scaling law

$$h_f(\lambda) = h_0^{D_T} \lambda^{1-D_T} \quad (4)$$

where D_T is the fractal dimension for tortuous capillaries/stream tubes, and D_T lies in the range of 1–2 in a 2D plane and 1–3 in 3D space. In eq 4, $h_f(\lambda)$ is the actual distance that fluid is imbibed, and $h_f(\lambda) \geq h_0$, and h_0 is the straight-line distance along the macroscopic pressure gradient.

Differentiating eq 4 with respect to time t for a single capillary results in^{26,43}

$$\nu_f = D_T h_0^{D_T-1} \lambda^{1-D_T} \nu_0 \quad (5)$$

where $\nu_f = dh_f/dt$ is the fractal/actual velocity of fluid flow in a tortuous capillary, and $\nu_0 = dh_0/dt$ is the straight-line imbibition velocity. Upon integration of eq 5 from the smallest pore/capillary to the largest one, the two average velocity relationships for fluid flow in a porous medium can be expressed as⁴³

$$\nu_0 = \left(\frac{D_T + D_f - 1}{D_T D_f h_0^{D_T-1} \lambda_{\min}^{1-D_T}} \right) \bar{\nu}_f \quad (6)$$

where $\bar{\nu}_f = d\bar{h}_f/dt$ is defined as the actual average velocity over all tortuous capillaries.

The total pore area (A_p) in porous media can be calculated by⁴⁰

$$A_p = \frac{\pi \lambda_{\max}^2 D_f}{4(2-D_f)} (1-\phi) \quad (7)$$

Based on the above fractal characters of pores and tortuous capillaries in porous media, the physical process of spontaneous capillary imbibition into gas-saturated porous media is analyzed in section 3.

3. Model for Spontaneous Imbibitions

Spontaneous imbibition experiments were usually performed by bringing the bottom face of a core sample into contact with wetting liquid. When the bottom surface of the sample (saturated with air) touches the liquid, the liquid is spontaneously imbibed into the sample. The core sample is kept vertical during the entire process. Zero initial wetting liquid saturation is usually assumed.

The flow rate for imbibed liquid through a single tortuous capillary with hydraulic diameter λ is governed by the Hagen–Poiseuille equation:

$$q(\lambda) = \frac{\pi}{128} \left(\frac{\Delta P}{h_f(\lambda)} \right) \left(\frac{\lambda^4}{\mu} \right) \quad (8)$$

where $h_f(\lambda)$ is the actual liquid imbibition distance/height, which increases with time in the imbibition process. In the imbibition process, the driving pressure difference (ΔP) is generated because of capillary action and is responsible for the liquid rising above the surface of the liquid in a container while acting against the weight of the column of liquid, so the modified pressure gradient ΔP may be expressed by

$$\Delta P = P_c - \rho g h_0 \quad (9)$$

where P_c , ρ , and h_0 are the capillary pressure, the density of fluid, and the straight rising height of fluid, respectively. From eq 9, it is seen that the pressure gradient ΔP decreases as the rising height increases. The capillary pressure is given by

$$P_c = \frac{4\sigma \cos \theta}{\lambda} \quad (10)$$

where σ is the surface tension and θ is the static contact angle used in the present work. From eq 10, it is seen that the capillary pressure is inversely proportional to the pore/capillary diameter.

Substituting eq 9 into eq 8 yields

$$q(\lambda) = \frac{\pi}{128} \left(\frac{P_c - \rho g h_0}{h_f(\lambda)} \right) \left(\frac{\lambda^4}{\mu} \right) \quad (11)$$

where P_c is determined by eq 10. The total imbibition rate (Q) can be obtained using the integral of all flow rates from the minimum to maximum capillaries as

$$Q = - \int_{\lambda_{\min}}^{\lambda_{\max}} q(\lambda) dN = \frac{\sigma \cos \theta}{32\mu} \left(\frac{\lambda_{\max}^{2+D_T}}{h_0^{D_T}} \right) \left[\frac{\pi D_f (1 - \beta^{2+D_T-D_f})}{2 + D_T - D_f} \right] - \frac{\rho g h_0}{128\mu} \left(\frac{\lambda_{\max}^{3+D_T}}{h_0^{D_T}} \right) \left[\frac{\pi D_f (1 - \beta^{3+D_T-D_f})}{3 + D_T - D_f} \right] \quad (12)$$

It can be seen from eq 12 that the total spontaneous imbibition rate is dependent on the imbibition height and on the structure parameters (D_f , D_T , λ_{\max} , and β) of porous media, fluid properties (μ , ρ , and σ), as well as the contact angle between the extraneous liquid and solid surface.

The average velocity of the rising front of the liquid in porous media can be obtained through $\bar{\nu}_f = Q/A_p$, i.e.,

$$\bar{\nu}_f = \frac{\sigma \cos \theta}{8\mu} \left(\frac{\lambda_{\max}^{D_T}}{h_0^{D_T}} \right) \left[\frac{(2-D_f)(1-\beta^{2+D_T-D_f})}{(2+D_T-D_f)(1-\phi)} \right] - \frac{\rho g h_0}{32\mu} \left(\frac{\lambda_{\max}^{1+D_T}}{h_0^{D_T}} \right) \left[\frac{(2-D_f)(1-\beta^{3+D_T-D_f})}{(3+D_T-D_f)(1-\phi)} \right] \quad (13)$$

(43) Yu, B. M.; Cai, J. C.; Zou, M. Q. *Vadose Zone J.* **2009**, *8*, 177–186.

Inserting eq 13 into eq 6 yields

$$\begin{aligned} \frac{dh_0}{dt} = & \frac{(D_T + D_f - 1)(2 - D_f)}{D_T D_f (2 + D_T - D_f)} \left(\frac{\sigma \cos \theta}{8\mu} \right) \\ & \left(\frac{\lambda_{\max}^{D_T}}{h_0^{2D_T-1} \lambda_{\min}^{1-D_T}} \right) \left(\frac{1 - \beta^{2+D_T-D_f}}{1 - \phi} \right) \\ & - \frac{(D_T + D_f - 1)(2 - D_f)}{D_T D_f (3 + D_T - D_f)} \left(\frac{\rho g h_0}{32\mu} \right) \left(\frac{\lambda_{\max}^{1+D_T}}{h_0^{2D_T-1} \lambda_{\min}^{1-D_T}} \right) \\ & \left(\frac{1 - \beta^{3+D_T-D_f}}{1 - \phi} \right) \end{aligned} \quad (14a)$$

For straight capillaries ($D_T = 1.0$), eq 14a can be simplified as

$$\begin{aligned} \frac{dh_0}{dt} = & \frac{2 - D_f}{3 - D_f} \left(\frac{\sigma \cos \theta}{8\mu} \right) \left(\frac{\lambda_{\max}}{h_0} \right) \left(\frac{1 - \beta^{3-D_f}}{1 - \phi} \right) \\ & - \frac{2 - D_f}{4 - D_f} \left(\frac{\rho g \lambda_{\max}^2}{32\mu} \right) \left(\frac{1 - \beta^{4-D_f}}{1 - \phi} \right) \end{aligned} \quad (14b)$$

Equations 14a and 14b are the differential expression for the liquid infiltration height. They show a linear relationship between the straight-line imbibition velocity (dh_0/dt) and the reciprocal of the imbibition height ($1/h_0$). From eq 14a, the imbibition height h_0 of the wetting liquid, as a function of time, can be obtained via numerical integration. It is also seen from eq 14a that the maximum imbibition height (h_m) can be found if we set $dh_0/dt = 0$, which yields

$$h_m = \frac{3 + D_T - D_f}{2 + D_T - D_f} \left(\frac{4\sigma \cos \theta}{\rho g \lambda_{\max}} \right) \left(\frac{1 - \beta^{2+D_T-D_f}}{1 - \beta^{3+D_T-D_f}} \right) \quad (15)$$

It may be noticed that the maximum imbibition height from eq 14a is different from that from eq 14b, because the fractal character of tortuosity is considered in eq 14a. Equation 15 indicates that the equilibrium height is not related to fluid viscosity.

For the initially short infiltration time, the second term on the right-hand side of eq 14a can be neglected; thus, after integration, we have

$$\begin{aligned} h_0^{2D_T} = & \frac{(D_T + D_f - 1)(2 - D_f)}{D_f (2 + D_T - D_f)} \left(\frac{\sigma \cos \theta}{4\mu} \right) \\ & \left(\frac{\lambda_{\max}^{D_T}}{\lambda_{\min}^{D_T-1}} \right) \left(\frac{1 - \beta^{2+D_T-D_f}}{1 - \phi} \right) t \end{aligned} \quad (16)$$

Equation 16 shows that the imbibition height follows a law of $h_0 \sim t^{1/(2D_T)}$, which is different from the LW behavior, which is described as $h_0 \sim t^{1/2}$. This is attributed to the fact that, in the present model, the fractal character of tortuous capillaries is considered. Zhao and Li²⁵ also found the imbibition height behavior is not 0.5, based on the fractal geometry.

Taking into account the kinematic relationships of the increase in the weight W due to the imbibition action, we have the weight W imbibed:

$$\begin{aligned} W = & A\phi\rho \int_{\lambda_{\min}}^{\lambda_{\max}} h_t(\lambda) f(\lambda) d\lambda \\ = & A\phi\rho \left(\frac{D_f h_0^{D_T} \lambda_{\min}^{1-D_T}}{D_T + D_f - 1} \right) \end{aligned} \quad (17)$$

Rewriting eq 17 yields

$$\frac{dW}{dt} = A\phi\rho \left(\frac{D_T D_f h_0^{D_T-1} \lambda_{\min}^{1-D_T}}{D_T + D_f - 1} \right) \frac{dh_0}{dt} \quad (18)$$

Inserting eq 14a into eq 18 and employing eq 17 yields

$$\begin{aligned} \frac{dW}{dt} = & \frac{(A\phi\rho)^2 D_f (2 - D_f)}{(2 + D_T - D_f)(D_T + D_f - 1)} \left(\frac{\sigma \cos \theta}{8\mu} \right) \\ & \left(\frac{\lambda_{\max}^{D_T}}{\lambda_{\min}^{D_T-1}} \right) \left(\frac{1 - \beta^{2+D_T-D_f}}{1 - \phi} \right) \left(\frac{1}{W} \right) \\ & - A\phi\rho \frac{2 - D_f}{3 + D_T - D_f} \left(\frac{\rho g h_0}{32\mu} \right) \left(\frac{\lambda_{\max}^{1+D_T}}{h_0^{D_T}} \right) \left(\frac{1 - \beta^{3+D_T-D_f}}{1 - \phi} \right) \end{aligned} \quad (19)$$

Equation 19 is a differential expression for the weight increase due to fluid imbibition. The imbibition weight of wetting liquid, as a function of time, can be obtained when the imbibition height is calculated from eq 19 via numerical integration.

For a straight capillary bundle ($D_T = 1.0$), eq 19 can be expressed as

$$\begin{aligned} \frac{dW}{dt} = & (A\phi\rho)^2 \left(\frac{2 - D_f}{3 - D_f} \right) \left(\frac{\lambda_{\max} \sigma \cos \theta}{8\mu} \right) \left(\frac{1 - \beta^{3-D_f}}{1 - \phi} \right) \frac{1}{W} \\ & - A\phi\rho \left(\frac{2 - D_f}{4 - D_f} \right) \left(\frac{\rho g \lambda_{\max}^2}{32\mu} \right) \left(\frac{1 - \beta^{4-D_f}}{1 - \phi} \right) \end{aligned} \quad (20)$$

Equations 19 and 20 show a linear relationship between dW/dt and $1/W$ with the straight line being not through the origin, and this is expected because the effect of gravitational force is considered in the present model.

Similarly, in an initially short period of imbibition time, the second term on the right-side of eq 19 can be neglected and then integration of eq 19 yields

$$\begin{aligned} W = & A\phi\rho \left[\frac{D_f (2 - D_f)}{(2 + D_T - D_f)(D_T + D_f - 1)} \left(\frac{\sigma \cos \theta}{4\mu} \right) \right. \\ & \left. \left(\frac{\lambda_{\max}^{D_T}}{\lambda_{\min}^{D_T-1}} \right) \frac{1 - \beta^{2+D_T-D_f}}{1 - \phi} \right]^{1/2} t^{1/2} \end{aligned} \quad (21)$$

Equation 21 shows that the accumulated imbibed weight in porous media is proportional to $t^{1/2}$ in the initial imbibition stage. This is consistent with the LW equation. From eq 21, it can be observed that the factors affecting the capillary imbibition include the structure parameters (D_f , D_T , λ_{\min} , λ_{\max} , β , ϕ , and A) of porous media, fluid properties (ρ , σ , μ), and the fluid–solid interaction (θ). However, the models by conventional methods cannot reveal such mechanisms, and therefore the present model may provide a better understanding of the mechanisms about imbibitions.

4. Results and Discussions

To discuss the proposed model for characterizing the spontaneous water imbibition into air-saturated porous media, the parameters of the proposed imbibition model are given as follows.

The pore fractal dimension (D_f) can be calculated as³⁷

$$D_f = d - \frac{\ln \phi}{\ln \beta} \quad (22)$$

where ϕ is the porosity and d is the Euclidean dimension (in this work, a value of $d = 2$ is used). The maximum pore diameter can be obtained based on the model of an equilateral-triangle arrangement of circular particles:³⁸

$$\lambda_{\max 1} = \frac{D_s}{2} \sqrt{\frac{2\phi}{1-\phi}} \quad (23a)$$

The maximum pore diameter also can be calculated based on the model of a square arrangement of circular particles:⁴⁴

$$\lambda_{\max 2} = \frac{D_s}{2} \left[\sqrt{\frac{\phi}{1-\phi}} + \sqrt{\frac{\pi}{4(1-\phi)}} - 1 \right] \quad (23b)$$

Thus, the average maximum pore diameter may be given as

$$\lambda_{\max} = \frac{\lambda_{\max 1} + \lambda_{\max 2}}{2} \quad (23c)$$

Equation 23c is an approximation for the maximum pore size. In reality, solid particles may be arranged in *neither* an equilateral-triangle arrangement *nor* a square arrangement in porous media, and the maximum pore size may change with rock types other than sandstones such as carbonates with other pore geometries and more heterogeneity in sizes. Therefore, a more realistic model for the maximum pore size in porous media is desirable. Unfortunately, no generally accepted model for the maximum pore size is presently available. Interested readers may consult a comprehensive review by Yu⁴⁵ for detail.

In eqs 23a and 23b, D_s is the mean diameter of particles, which can be predicted based on the rearranged Kozeny–Carman equation:⁴⁵

$$D_s = \frac{4(1-\phi)}{\phi} \sqrt{\frac{Kk}{\phi}} \quad (24)$$

where K is the permeability, and the Kozeny constant (k) is equal to 4.8 ± 0.3 .

The value of D_T is determined by⁴⁶

$$D_T = 1 + \frac{\ln \tau_{av}}{\ln(L_0/\lambda_{av})} \quad (25)$$

where λ_{av} and τ_{av} are the average pore/capillary size and the averaged tortuosity, respectively. The parameters τ_{av} and L_0/λ_{av} can be found using the expressions^{46,47}

$$\tau = \frac{1}{2} \left[1 + \frac{1}{2} \sqrt{1-\phi} + \frac{\sqrt{(\sqrt{1-\phi}-1)^2 + (1-\phi)/4}}{1-\sqrt{1-\phi}} \right] \quad (26)$$

$$\frac{L_0}{\lambda_{av}} = \frac{D_f - 1}{2\beta} \sqrt{\left(\frac{1-\phi}{\phi}\right) \left(\frac{\pi}{D_f(2-D_f)}\right)} \quad (27)$$

It was generally recognized^{46,47} that the minimum pore size is 2 orders of magnitude smaller than the maximum pore size in

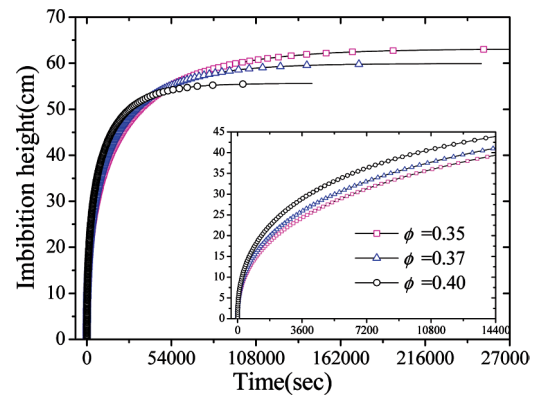


Figure 1. Plot of imbibition height versus the time of imbibition at different porosities through numerical integration of eq 14a.

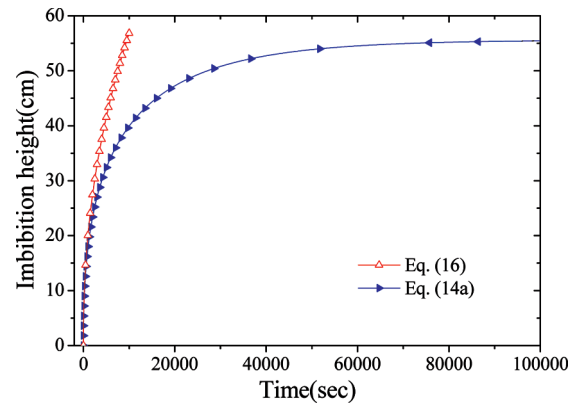


Figure 2. Comparison of the effect of gravity factor on the imbibition height based on eq 14a and eq 16 at $\phi = 0.4$.

porous media. Therefore, the expression $\beta = \lambda_{\min}/\lambda_{\max} = 0.01$ (taken from ref 37) is used in this work. Thus, when K , k , and ϕ are given, and the parameters D_f , D_T , and λ_{\max} are determined, the imbibition height and weight can be calculated using the proposed expressions.

In this work, water is considered to be an imbibition liquid, and the relevant parameters $\sigma = 0.0727$ N/m, $\rho = 1.0$ g/cm³, $\mu = 0.001$ Pa s, $\theta = 30^\circ$, and $D_s = 0.02$ cm are used in the following discussions. The maximum pore sizes at different porosities are calculated using eq 23c, and the fractal dimensions D_f and D_T are determined by eqs 22 and 25, respectively.

The imbibition height versus structure parameters is shown in Figures 1–3. Figure 1 plots the imbibition height versus time of imbibition at different porosities through numerical integration of eq 14a. The imbibition height increases rapidly in the initial period of imbibition time and then increases more slowly and approaches the equilibrium, which takes a long time for the wetting liquid. From Figure 1, it is seen that the higher equilibrium height corresponds to lower porosity. Also note that a decrease in porosity is responsible for a decrease in the capillary imbibition rate and the imbibition takes more time to approach the equilibrium (see the inset in Figure 1). This phenomenon may be explained in more detail that lower porosity generally leads to lower permeability, meaning smaller pore throats, which will generate a larger capillary pressure, leading to faster capillary imbibition rates. However, as the pore throats become smaller, flow becomes more difficult, so there is a balance between these two properties.

Figure 2 shows a slight difference between the predictions by eq 14a (the gravity is included) and by eq 16 (the gravity

(44) Wu, J. S.; Yu, B. M. *Int. J. Heat Mass Transfer* **2007**, *50*, 3925–3932.

(45) Carman, P. C. *Trans. Inst. Chem. Eng.* **1937**, *15*, 150–167.

(46) Yu, B. M.; Li, J. H. *Chin. Phys. Lett.* **2004**, *21*, 1569–1571.

(47) Xu, P.; Yu, B. M. *Adv. Water Resour.* **2008**, *31*, 74–81.

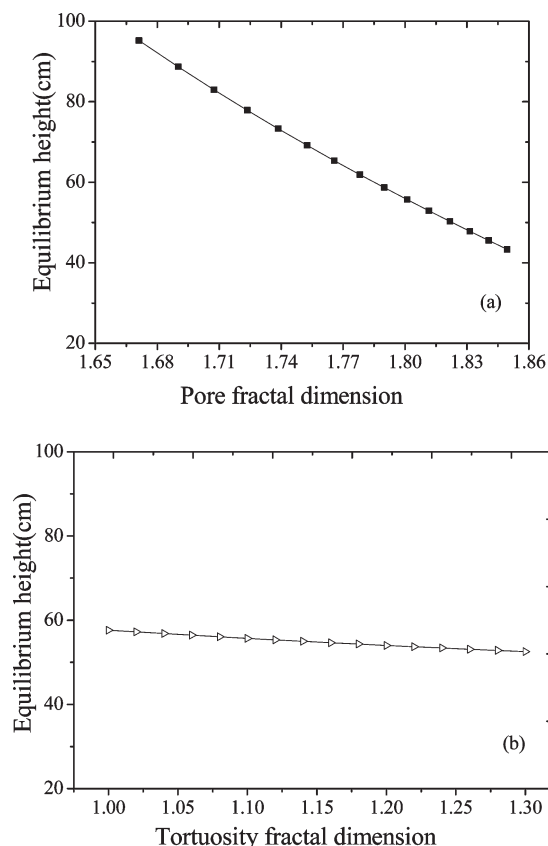


Figure 3. Plot of the equilibrium height versus the fractal dimensions (a) for pores and (b) for tortuosity, based on eq 15.

is neglected) at the early imbibition time. This validates that the gravity factor can be neglected in the early period of imbibition time. However, the gravity factor may have significant influence on the imbibition height after ~ 2500 s, at which the imbibition height predicted by eq 16 is much higher than that by eq 14a and quickly tends to infinity. Therefore, the imbibition height predicted by eq 14a may be more reasonable than eq 16 and the gravity factor should be taken into account.

Figure 3 shows that the equilibrium height changes with fractal dimensions for pores (D_f) and for tortuosity (D_T), based on eq 15. Figure 3a shows that the pore fractal dimension has a significant effect on the equilibrium height. This can be explained by the fact that the equilibrium height is significantly dependent on porosity, while the pore fractal dimension is also significantly dependent on porosity. However, the tortuosity fractal dimension has slight influence on the equilibrium height, as shown in Figure 3b. The fractal dimension for tortuosity of tortuous capillaries represents the heterogeneity of real porous rocks, and the larger fractal dimension corresponds to a more-heterogeneous medium, which has a lower capillary imbibition equilibrium height.

To verify the validity of the proposed model, the theoretical predictions are tested using the available experimental data.^{4,9,48} The comparisons of the model predictions for imbibition weight with the experimental results are shown in Figures 4–6. Water was used as the imbibed liquid in these experiments ($\sigma = 0.0727$ N/m, $\rho = 1.0$ g/cm³, and $\mu = 0.001$ Pa s). The unconsolidated porous medium (glass-bead pack) was

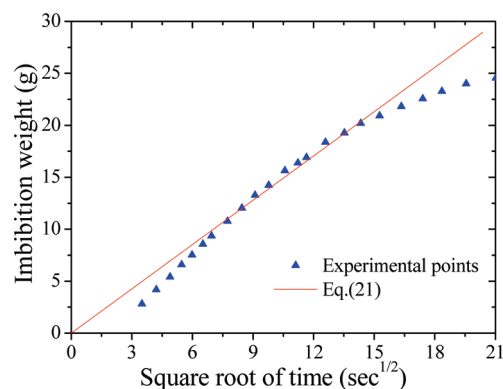


Figure 4. Comparison of the weight of water imbibed versus the square root of imbibition time by the present model predictions (based on eq 21) with the experiment data.⁴

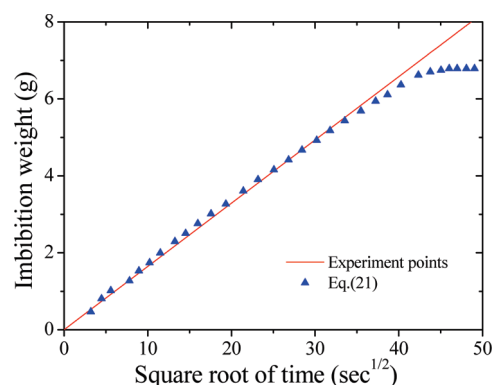


Figure 5. Comparison of the model predictions (based on eq 21) of the weight water imbibed versus the square root of imbibition time with the experiment data.⁹

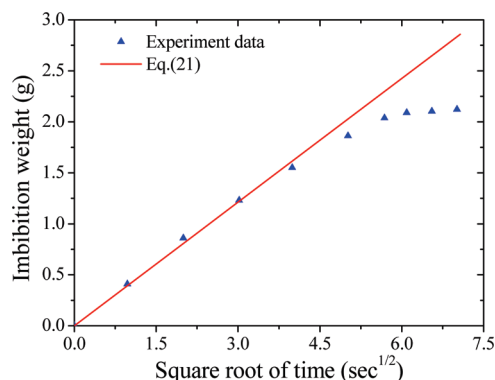


Figure 6. Comparison of the spontaneous imbibition weight of water versus the square root of imbibition time by the model predictions (based on eq 21) with the experiment data⁴⁸ at a porosity of 0.23.

used as the core sample in Li and Horne's measurements,⁴ and the consolidated porous media (Berea sandstone and Bentheim) were used in the experiments of Schembre et al.⁹ and Olafuyi et al.⁴⁸ In all cases, the experiments were conducted under isothermal conditions. The detailed sample characteristics are listed in Table 1.

In Figures 4–6, Kozeny constants of $k = 4.6$, 5.1, and 5.5 were respectively applied to fit the experimental data in Figure 4 for the glass-bead pack sample, Figure 5 for Berea sandstone sample, and Figure 6 for Bentheim core. In all of

(48) Olafuyi, O. A.; Cinar, Y.; Knackstedt, M. A.; Pinczewski, W. V. SPE Paper No. 109724. Presented at Asia Pacific Oil and Gas Conference and Exhibition, Jakarta, Indonesia, October 30–November 1, 2007.

Table 1. Rock Sample Characteristics and the Contact Angles with Water on Surfaces

rock type	shape	length (cm)	diameter (cm)	porosity (%)	permeability (Darcy)	contact angle (°)
glass-bead pack ⁴	cylindrical	29.5	3.40	38.6	25.7	50
Berea ⁹	cylindrical	11.0	2.00	15.0	0.5	26
Bentheim ⁴⁸	cylindrical	2.56	2.56	23.0	2.89	0

these comparisons, the Kozeny constants are comparable to a value of 4.8 ± 0.3 .⁴⁵

Before the imbibition front reaches a certain height above the level of the water surface of a container, the imbibition process is a capillary pressure-dominating process as assumed in the model derivation. In Figures 4–6, it can indeed be seen that the experimental results clearly exhibit a linear relationship at the initial period of imbibed time. It is worth noting that the initial period of imbibition time with a linear relationship is different in each case. For example, the time period is ~ 400 s in Figure 4, ~ 1600 s for the Berea sandstone sample (as shown in Figure 5), and ~ 30 s for the Bentheim core (depicted in Figure 6). This may be due to the different pore structure and permeability, as well as the wettability of rock samples.

In Figure 4, the imbibed volume/weight is linear until a time of 400 s, before constantly decreasing as $t^{1/2}$ progresses. The model overestimates the imbibition rate at the start and end of the test. The fit between the model and the experimental data is improved in Figures 5 and 6, where the volume is linear with $t^{1/2}$. This verifies the validity of the theoretical predictions by eq 21. It is observed that the amount of imbibed water is linearly dependent on the square root of time in some period of imbibition time. In fact, the effect of gravity on the imbibition process increases with the increase of height of the imbibition front.⁴ Thus, after a certain period of imbibition time, the influence of gravity becomes increasingly important. In addition to increasing gravity, the driving capillary pressure must pull the water from the basin further up the core as the front progresses upward; i.e., more and more of the capillary pressure is consumed in transporting the water upward. Thus, the imbibition rate slows with time and causes deviation of the measured points from the straight line (see Figures 4–6).

Also note that, in Figure 4, the experiment points in the initial period of imbibition time do not go through the origin. Li and Horne⁴ explained that this phenomenon might be caused by gravity and several other reasons: (a) because of the influence of the buoyancy caused by inserting the core sample into the water in a container, data from the early spontaneous imbibition into porous media are usually difficult to record accurately; and (b) the core sample may not be fully submerged in water and thus causes the water to not be imbibed immediately. In addition, the imbibition rate at the immediate start of the test is not necessarily required to be linear with $t^{1/2}$, because some counter-current imbibition occurs at the start. The mode of imbibition switches to co-current after some period of imbibition time.

5. Conclusions

We have shown analytical models (eq 14a for imbibition height, eq 19 for imbibition weight in which the gravitational factor is included, and eq 21 for imbibition weight in which the gravitational factor is excluded) for spontaneous imbibition of wetting fluid into gas-saturated porous media by considering the fractal characters of pores and capillaries in porous media. The imbibition rate decreases with time, primarily because the gravity increases with the height of the imbibition front. The imbibition mass/weight is dependent on

pore/capillary size (λ_{\min} , λ_{\max} , and β), porosity (ϕ), cross-sectional area (A), fractal dimensions (D_f and D_T) of pores and capillaries in porous media, and fluid properties (σ , μ , and ρ), as well as liquid–solid interaction (θ).

The model described by eq 21 has been verified by predicting the accumulated imbibition weight into water-wet porous media in the initial period of imbibition time. The predictions of imbibition weight are compared and show good agreement with the published results. Knowledge of fluid properties and structure characters can immediately predict the imbibition into homogeneous porous media based on the proposed model without calculating the permeability of porous media and capillary pressure. It is worth emphasizing that eq 21 is only applicable to the initially short period of imbibition time, which varies with the specific types of porous media, because, as time approaches infinity, the imbibition rate according to eq 21 continuously increases and approaches infinity. This is physically unrealistic. For an entire imbibition period, the gravity factor should be included, and the spontaneous capillary imbibition weight can be obtained by numerical integration of eq 19.

It is expected that the proposed model may have potential in the analysis of oil–water systems as long as the fluid properties and microstructural parameters of a porous medium have been determined.

Acknowledgment. This work was supported by the National Natural Science Foundation of China (through Grant No. 10932010).

Nomenclature

Parameters

- A = cross-section area of the core (cm²)
- A_p = total pore area (cm²)
- d = Euclidean dimension
- D_s = mean diameter of particles (cm)
- D_f = pore fractal dimension
- D_T = fractal dimension for tortuous capillaries/stream-tubes
- h_0 = straight-line distance along the macroscopic pressure gradient (cm)
- h_f = actual distance that fluid is imbibed (cm)
- k = Kozeny constant
- K = effective permeability (Darcy)
- P_c = capillary pressure (Pa)
- Q = total imbibition rate (mL/min)
- S_{wf} = wetting phase saturation (fraction)
- t = imbibition time (s)
- W = mass of wetting fluid imbibed (g)

Abbreviations

- LW = Lucas–Washburn equation

Greek Symbols

- β = ratio of the minimum pore size to maximum pore size
- ΔP = pressure gradient (Pa)
- λ = pore/capillary diameter (cm)

λ_{av} = average pore/capillary size (cm) λ_{max} = maximum pore size (cm) λ_{min} = minimum pore size (cm) μ = viscosity (Pa s) ν_0 = straight-line imbibition velocity (cm/s) ν_f = fractal/actual velocity of fluid flow in a tortuous capillary (cm/s) $\bar{\nu}_f$ = actual average velocity over all tortuous capillaries (cm/s) θ = contact angle (°) ϕ = porosity (fraction) ρ = density (g/cm³) σ = surface tension (N/m) τ_{av} = average tortuosity